

Title: Direct Observation of Coronal Magnetic Reconnection leading to a Solar Flare

Authors: Yang Su^{1*}, Astrid Veronig¹, Brian R. Dennis², Gordon D. Holman², Tongjiang Wang^{2,3}, Manuela Temmer¹, Weiqun Gan⁴

Affiliations:

¹Kanzelhöhe Observatory-IGAM, Institute of Physics, University of Graz, Universitaetsplatz 5/II, Graz 8010, Austria.

²Solar Physics Laboratory (Code 671), Heliophysics Science Division, NASA Goddard Space Flight Center, Greenbelt, MD 20771, USA.

³Department of Physics, the Catholic University of America, Washington, DC 20064, USA.

⁴Key Laboratory of Dark Matter and Space Astronomy, Purple Mountain Observatory, Chinese Academy of Sciences, Nanjing 210008, China.

*Correspondence and requests for materials should be addressed to Y. S. (yang.su@uni-graz.at).

Abstract:

Magnetic field reconnection is believed to play a fundamental role in magnetized plasma systems throughout the universe¹, including planetary magnetospheres, magnetars, and accretion discs around black hole, but never before has it been so clearly demonstrated as in the EUV and X-ray movies of a GOES-class C2.3 solar flare presented in this letter. The multiwavelength EUV observations from SDO/AIA show the predicted inflowing cool loops and newly formed outflowing hot loops while simultaneous RHESSI X-ray spectra and images show the appearance of plasma heated to >10 MK at the expected locations. These two data sets provide solid visual evidence of magnetic reconnection producing a solar flare. The non-uniform, non-steady, and asymmetric nature of the observed process, together with the measured reconnection rates, supports the so called flux-pile-up reconnection² rather than the classic Petschek reconnection³. These new features of plasma inflows should be included in reconnection and flare studies.

Main Text:

Reconnection process reconfigures the field topology and converts magnetic energy to thermal energy, mass motions, and particle acceleration. The theories and related numerical simulations are still the subjects of extensive research towards a full understanding of the process under different conditions, especially the full 3D modelling. Meanwhile, observational studies have made progress in searching for evidence of reconnection and deriving its physical properties to constrain and improve the theories. In-situ measurements of the magnetic field, plasma parameters, and particle distributions have shown the existence of magnetic reconnection in laboratory plasmas, fusion facilities^{4,5}, and magnetospheres of planets⁶⁻⁸. In the hot, dynamic solar atmosphere, considerable pieces of evidence for features likely to be related to reconnection have been obtained in solar flares and coronal mass ejections (CMEs⁹) by remote sensing of the emissions at different wavelengths from radio to X-rays and gamma rays^{10,11}. These include signatures of plasma inflow and outflow¹²⁻¹⁶, hot cusp structures¹⁷, current sheets¹⁸⁻²¹, fast-mode standing shocks²², and plasmoid ejection²³. However, most evidence has been indirect and fragmented. Detailed observations of the complete picture are still missing due to the highly dynamic flare/CME process and limited observational capabilities.

The situation was significantly improved by the launch of the Solar Dynamic Observatory (SDO²⁴) in 2010. In particular, the Atmospheric Imaging Assembly (AIA²⁵) has enabled continuous imaging of the full Sun in ten EUV, UV, and visible channels, with a spatial resolution of ~ 0.6 arcsec and a cadence of 12 s. Simultaneously, the Ramaty High Energy Solar Spectroscopic Imager (RHESSI²⁶) is continuing to provide X-ray imaging and spectroscopic diagnostics of the heated plasma and accelerated electrons in flares. The combination of SDO and RHESSI data presented here provides the first complete picture yet obtained of the magnetic reconfiguration and energy release in an interacting coronal loop arcade leading to a flare.

The transition of magnetic topology from a horizontally reconnecting magnetic arcade of loops into two vertically-separated loop systems was observed close to the southeast limb on 2011 August 17. From ~04:05 UT to 04:28 UT, coronal loops seen in relatively cooler AIA channels (from ~0.05 MK to 2 MK), such as 171, 193, 211 and 304 Å, moved towards one another and disappeared near a central line, where an “X”-shaped structure gradually formed by 04:10 UT in the hot AIA channels, 94 (6.3 MK) and 131 (temperature response peaks at 0.4, 10, and 16 MK) Å (see Fig. 1 and particularly the supplementary movies M1-M3). In fact, some inflow loops pass through one another and do not disappear at the same location, suggesting that the reconnection occurred in different planes along the loop arcade which is at an oblique angle to the line of sight. The first major group of loops reached the central line at ~04:10 UT, when the pre-existing loops appeared to shrink. Meanwhile, the two cusp-like structures above and below the X-point began to separate to form a double-Y-structure at ~04:15 UT. Large, newly formed loops with a temperature > 6 MK connecting the higher reversed-cusp and the surface expanded while the hot loops below the X-structure shrank with the lower cusp (Fig. 1c and supplementary movie M2). The magnetic topology likely changed from the loops connecting the lettered ribbons AB and CD in Fig. 1 to AC and BD (see also Fig. 2 and supplementary Fig. 1).

X-ray observations of energy release confirm the reconnection process between the inflowing loops. The C2.3 (1-8 Å) flare was recorded by GOES and RHESSI (Fig. 3c) with no detectable CME. The RHESSI X-ray flux began to increase at 04:06:40 UT, close to the time when the EUV inflow loops visibly started moving together. The GOES 1-8 Å flux peaked at 04:29 UT, the time when the last inflow loops were seen disappearing (Fig. 3d). On the other hand, X-ray images and spectra show hot X-ray sources (from ~6 MK to 17 MK, Fig. 2c) at the same location as the EUV flare loops in addition to other coronal sources. When the X-structure

formed, RHESSI detected a coronal source in the 4-10 keV energy range at the same location (Fig. 4b), indicating the presence of plasma at ~ 6 MK. After 04:19 UT, a high coronal source appeared in the 10–20 keV images above the higher, relaxing cusp (Fig. 2b and Fig. 4b). The two coronal X-ray sources, i.e. the cusp-like extended source above the flare loops and the higher coronal source, together with the EUV observations strongly suggest heating in the outflow regions above and below a current sheet in between, similar to the interpretation proposed when they were first discovered in RHESSI images alone for a different flare¹⁸. It is also consistent with the simulation results on the heating and density enhancements in contracting loops flowing away from a reconnection site²⁷.

In order to quantitatively investigate the inflow and outflow motions evident in the EUV movies, we defined two curves labelled C1 and C2 in Fig. 1. The resulting time-distance plots for C1 (Fig. 3a) show coronal loops from both sides moved together and disappeared. The apparent inflow velocities increased from ~ 10 to over 50 km s^{-1} as the loops approached the point of disappearance. The final inflow velocities (V_{in}) range from 20 to $\sim 70 \text{ km s}^{-1}$. The time-distance plots for C2 are designed to reveal the outflows which are evident in the plots made from the 131 Å images (Fig. 3). Some signatures can be seen in the filtered stack plot along the paths of the two separating cusps (two dashed cyan lines in Fig. 3d), which were superposed by some fast moving structures from 04:08 to 04:22 UT. We suggest that these structures are the ejecting new loops and that the two cusps are thermal sources of plasma heated by the reconnection. The initial outflow velocities (V_{out}) range from ~ 90 to $\sim 440 \text{ km s}^{-1}$.

The highly curved inflow loops expanded as they approached the reconnection site. Using Fourier Local Correlation Tracking (FLCT²⁸), we derived detailed flow velocity maps (Fig. 4) to quantify this expansion. According to the 2D reconnection theory¹, diverging inflows

indicate a flux-pile-up reconnection. Other regimes resulting from different boundary conditions include Sweet-Parker-like, Petschek-like, Sonnerup-like, stagnation-point flow, and Strachan-Priest reconnection. They differ not only in inflow pattern but also in reconnection rates, $M \cong V_{in}/V_{out}$, a factor that tells us whether the regime can explain the high rate of energy conversion measured in various plasma systems. The calculated reconnection rates in this event vary from ~ 0.05 to 0.6 (Fig. 3e). Note that the true final inflow velocity could be higher than the values used here due to acceleration of the inflow and/or projection effects, leading to even higher reconnection rates. Most values significantly exceed the maximum rate of ~ 0.1 that Petschek-like reconnection could reach but can be explained by flux-pile-up reconnection¹. A third piece of evidence supporting flux-pile-up reconnection arises from the stack plots for AIA 171 Å (white arrows in Fig 3a), where pile-up loops at $\sim 04:16$ UT showed higher intensity than the inflowing loops.

The event showed other new features of inflows. Some inflow loops originated far from the reconnection site (up to $40''$). They were visible in different AIA channels and hence must have covered a wide range of temperatures from ~ 0.05 to at least 2 MK. Consequently, they may have had different physical states from that of the initial local plasma at the reconnection site. Thus, the inflows appeared curved and variable. Compared with the steady, uniform case, these loops would cause temporally enhanced reconnection rates, which may help explain the spikes observed in hard X-rays during the impulsive phase of many flares.

Furthermore, the reconnection was apparently asymmetric. The apparent inflow velocities at $04:20-21$ UT were ~ 50 km s⁻¹ from the south and ~ 20 km s⁻¹ from the north. This difference could be due to different viewing angles of the incoming loops or different magnetic field strength on the two sides. Since the reconnection process consumes the same amount of

opposite magnetic fluxes $|V_{in_S}|B_S = |V_{in_N}|B_N$ from the two inflow regions, one would expect that a weaker field requires a faster inflow speed. Then the region with the weaker field would thus be the region to the south. It would project down to the chromosphere over a larger area²⁹ and produce a stronger X-ray footpoint because of the weaker magnetic mirroring effect, allowing more non-thermal electrons to reach the footpoint and emit hard X-rays. The measured ratio of X-ray fluxes in 10-20 keV in the southern and northern footpoints is $\sim 3:1$; the ratio of newly brightened footpoint areas (pixels with intensity above $300 \text{ DN s}^{-1} \text{ pixel}^{-1}$) in the 1600 \AA images is $\sim 2:1$. Thus, all the measurements support a weaker magnetic field in the southern ribbon within this time range.

The early phase of this event before $\sim 04:20$ UT showed a complete picture expected from the 2D reconnection model. However, the later phase became more complicated. This may have resulted from reconnection in 3D space, where loops in other magnetic domains could also be dragged into the reconnection region¹⁵. Large-scale 3D simulations are required extending through these more complex stages to better understand the longer term reconnection processes in the solar corona.

References:

1. **Priest, E. and Forbes, T.** *Magnetic Reconnection*. Cambridge : Cambridge University Press , 2000.
2. *New models for fast steady state magnetic reconnection*. **Priest, E. R. and Forbes, T. G.** 1986, J. Geophys. Res., 91, 5579-5588 (1986).
3. *Magnetic Field Annihilation*. **Petschek, H. E.** [ed.] Wilmot N. Hess. Washington, DC, US : National Aeronautics and Space Administration, Science and Technical Information Division, 1964. The Physics of Solar Flares, Proceedings of the AAS-NASA Symposium held 28-30 October, 1963 at the Goddard Space Flight Center, Greenbelt, MD, 425 (1964).
4. *Magnetic reconnection*. **Yamada, M., Kulsrud, R. and Ji, H. T.**, Rev. Mod. Phys., 82, 603-664 (2010).
5. *Modelling loop-top X-ray source and reconnection outflows in solar flares with intense lasers*. **Zhong, Jiayong; Li, Yutong; Wang, Xiaogang; Wang, Jiaqi; Dong, Quanli, et al.**, Nature Physics, 6, 984-987 (2010).
6. *Rapid magnetic reconnection in the Earth's magnetosphere mediated by whistler waves*. **Deng, X. H. and Matsumoto, H.**, Nature, 410, 557-560 (2001).

7. *In situ detection of collisionless reconnection in the Earth's magnetotail.* **Øieroset, M.; Phan, T. D.; Fujimoto, M.; Lin, R. P.; Lepping, R. P.**, Nature, 412, 414-417 (2001).
8. *Magnetic Reconnection in the Near Venusian Magnetotail.* **Zhang, T. L.; Lu, Q. M.; Baumjohann, W.; Russell, C. T.; Fedorov, A., et al.**, Science, 336, 567 (2012).
9. *Coronal Mass Ejections: Models and Their Observational Basis.* **Chen, P. F.**, Living Reviews in Solar Physics, 8, 1 (2011).
10. *An Observational Overview of Solar Flares.* **Fletcher, L.; Dennis, B. R.; Hudson, H. S.; Krucker, S.; Phillips, K., et al.**, Space Sci. Rev., 159, 19-106 (2011).
11. *Solar Flares: Magnetohydrodynamic Processes.* **Shibata, K. and Magara, T.**, Living Reviews in Solar Physics, 8, 6 (2011).
12. *Clear Evidence of Reconnection Inflow of a Solar Flare.* **Yokoyama, T.; Akita, K.; Morimoto, T.; Inoue, K.; Newmark, J.**, Astrophys. J., 546, L69-L72 (2001).
13. *Observations of the Magnetic Reconnection Signature of an M2 Flare on 2000 March 23.* **Li, L. P. and Zhang, J.**, Astrophys. J., 703, 877-882 (2009).
14. *Direct Observation of High-Speed Plasma Outflows Produced by Magnetic Reconnection in Solar Impulsive Events.* **Wang, T. J., Sui, L. H. and Qiu, J.**, Astrophys. J., 661, L207-L210 (2007).
15. *Low-altitude Reconnection Inflow-Outflow Observations during a 2010 November 3 Solar Eruption.* **Savage, S. L.; Holman, G.; Reeves, K. K.; Seaton, D. B.; McKenzie, D. E., et al.**, Astrophys. J., 754, 13 (2012).
16. *Simultaneous Observation of Reconnection Inflow and Outflow Associated with the 2010 August 18 Solar Flare.* **Takasao, S.; Asai, A.; Isobe, H.; Shibata, K.**, Astrophys. J., 745, L6 (2012).
17. *Observation of a solar flare at the limb with the YOHKOH Soft X-ray Telescope.* **Tsuneta, S.; Hara, H.; Shimizu, T.; Acton, L. W.; Strong, K. T.; et al.**, Publ. Astron. Soc. Jpn., 44, L63-L69 (1992).
18. *Evidence for the Formation of a Large-Scale Current Sheet in a Solar Flare.* **Sui, L. H. and Holman, G. D.**, Astrophys. J., 596, L251-L254 (2003).
19. *Direct Observations of the Magnetic Reconnection Site of an Eruption on 2003 November 18.* **Lin, J.; Ko, Y.-K.; Sui, L.; Raymond, J. C.; Stenborg, G. A., et al.**, Astrophys. J., 622, 1251-1264 (2005).
20. *Episodic X-Ray Emission Accompanying the Activation of an Eruptive Prominence: Evidence of Episodic Magnetic Reconnection.* **Liu, W.; Wang, T. J.; Dennis, B. R.; Holman, G. D.**, Astrophys. J., 698, 632-640 (2009).
21. *A Reconnecting Current Sheet Imaged in a Solar Flare.* **Liu, R.; Lee, J.; Wang, T. J.; Stenborg, G.; Liu, C., et al.**, Astrophys. J., 723, L28-L33 (2010).
22. *A loop-top hard X-ray source in a compact solar flare as evidence for magnetic reconnection.* **Masuda, S.; Kosugi, T.; Hara, H.; Tsuneta, S.; Ogawara, Y.**, Nature, 371, 495-497 (1994).
23. *Observations of X-ray jets with the YOHKOH Soft X-ray Telescope.* **Shibata, K.; Ishido, Y.; Acton, L. W.; Strong, K. T.; Hirayama, T., et al.**, Publ. Astron. Soc. Jpn., 44, 173-179 (1992).
24. *The Solar Dynamics Observatory (SDO).* **Pesnell, W. D., Thompson, B. J. and Chamberlin, P. C.**, Sol. Phys., 275, 3-15 (2012).
25. *The Atmospheric Imaging Assembly (AIA) on the Solar Dynamics Observatory (SDO).* **Lemen, J. R.; Title, A. M.; Akin, D. J.; Boerner, P. F.; Chou, C., et al.**, Sol. Phys., 275, 17-40 (2012).
26. *The Reuven Ramaty High-Energy Solar Spectroscopic Imager (RHESSI).* **Lin, R. P.; Dennis, B. R.; Hurford, G. J.; Smith, D. M.; Zehnder, A., et al.**, Sol. Phys., 210, 3-32 (2002).
27. *A Model for the Origin of High Density in Looptop X-Ray Sources.* **Longcope, D. W. and Guidoni, S. E.**, Astrophys. J., 740, 73 (2011).
28. *FLCT: A Fast, Efficient Method for Performing Local Correlation Tracking.* **Fisher, G. H. and Welsch, B. T.** [ed.] R. W. Komm, K. S. Balasubramaniam and G. J. D. Petrie R. Howe. San Francisco : Astronomical Society of the Pacific, Subsurface and Atmospheric Influences on Solar Activity ASP Conference Series. 383, 373 (2008).

29. *Motion of Flare Footpoint Emission and Inferred Electric Field in Reconnecting Current Sheets.* Qiu, J.; Lee, J.; Gary, D. E.; Wang, H. M., *Astrophys. J.*, 565, 1335-1347 (2002).
30. *Analysis of RHESSI Flares Using a Radio Astronomical Technique.* Schmahl, E. J.; Pernak, R. L.; Hurford, G. J.; Lee, J.; Bong, S., *Sol. Phys.*, 240, 241-252 (2007).
31. *Comparison of Solar X-Ray Line Emission with Microwave Emission during Flares.* Neupert, W. M., *Astrophys. J.*, 153, L59 (1968).

Acknowledgments:

The authors dedicate this paper to the RHESSI (Ramaty High Energy Solar Spectroscopic Imager) PI, Robert P. Lin, recently deceased, in acknowledgement of his inspirational efforts that made possible the high quality solar X-ray data used in this paper. RHESSI is a NASA Small Explorer Mission. The Solar Dynamics Observatory (SDO) is a mission for NASA's Living With a Star (LWS) Program. The work of Y.S. and A.V. was supported by the European Community Framework Programme 7, High Energy Solar Physics data in Europe (HESPE), grant agreement No. 263086. Y. S. also acknowledges NSFC 11233008. The work of G. H. was supported by a NASA Guest Investigator Grant and the RHESSI program. The work of TW was supported by NASA grant NNX12AB34G and NASA Cooperative Agreement NNG11PL10A to CUA. M.T. acknowledges the Austrian Science Fund (FWF): V195-N16. W. G. acknowledges 2011CB811402 and NSFC 11233008.

Y. S. analysed the data, wrote the text and led the discussion. A. V., B. D., G. H., T. W., M. T. and W. G. contributed to the interpretation of the data. All authors helped improving the manuscript.

The authors declare no competing financial interests.

Fig. 1. SDO/AIA observations of the inflowing and outflowing loops on 2011 August 17. (a)

AIA images at 211, 193, 171 and 304 Å show inflow loops with temperatures from ~0.05 to 2 MK. The X and Y coordinates are in arcsecond (~735 km) from the center of the visible solar disk. The white curved lines mark the visible edge of solar disk. The white box in the third image indicates the field of view for Fig. 4. (b) Same as images shown in (a) after subtracting images taken one minute earlier. These difference images show moving, brightened inflow loops and structures in white relative to their original positions in black. The red line marks the initial location of the X-structure where the inflow loops appeared to come together and disappear. The red arrows show the inflow directions. (c) AIA images at 131 Å showing plasma structures hotter than 10 MK. The yellow dashed curves marked C1 and C2 are used to derive the inflow and

outflow profiles shown in Fig. 3. The flare ribbons (pink, marked by A, B, C and D, see also supplementary Fig. 1) observed in AIA 1600 Å images are superposed in the third image. The two red arrows in the third image show the flow directions of the hot, separating loops. See also the supplementary movies M1, M2 and M3.

Fig. 2. The reconnection process and energy release imaged by SDO/AIA in EUV and RHESSI in X-rays. (a) AIA 131 Å images taken on August 17, 2011, at the indicated times show the evolution of the hot, newly formed loops. The images are rotated clockwise by 114° to orient the limb (shown as the thin black line in each image) in the horizontal direction. (b) RHESSI X-ray sources in the 4-10 (red) and 10-20 (blue) keV bands are shown at contour levels of 10, 20, 40, 60, and 90 percent of the maximum in each image made from detectors 4 through 9 using the MEM-NJIT image reconstruction algorithm³⁰. Orange lines show the major inflow loops defined from both original and filtered AIA images at 171, 193, 211 and 304 Å, and cyan lines the hot flaring loops and cusps in AIA 131 Å images. Flare ribbons visible in AIA images at 1600 Å with fluxes of $>300 \text{ DN s}^{-1} \text{ pixel}^{-1}$ are shown in pink. The combination of data from different wavelengths/temperatures shows the whole sequence of events expected for reconnection. The dashed grey lines (in the last image) show the likely loop connections A-B and C-D before the reconnection and the solid grey lines show the newly formed loops A-C and B-D after the reconnection. Arrows indicate the flow direction. (c) RHESSI X-ray photon spectra from the heated plasma. The background-subtracted spectra ($\text{photons s}^{-1} \text{ cm}^{-2} \text{ keV}^{-1}$) obtained from detector 3 are shown as histograms with error bars. The integration time for each spectrum is one minute. Two isothermal components (red and green) are used to fit the spectra. The obtained temperatures (T) are indicated in the plots. See also supplementary movie M4.

Fig. 3. Time profiles of plasma inflow, plasma outflow, and X-ray flux. (a) Time-distance plots (stack plots) showing (from the top) the time history of the intensity along curve C1 in AIA images at 171, 193, 211, and 304 Å, and along C2 at 131 Å (Curves C1 and C2 are shown in the second image of Fig. 1c). The white arrows in the first row indicate the signature of piled-up loops. (b) Filtered images of the stack plots on the left to more clearly show the loop motions. (c) RHESSI X-ray light curves in the 3-6, 6-12, and 12-25 keV bands, and GOES X-ray light curves in the 1-8 and 0.5-4 Å channels. (d) Signatures of inflow (orange) and outflow (cyan) indicated in the stack plots shown above. The grey curve shows the time derivative (times 30,000) of GOES 1-8 Å flux as a proxy of the flare heating rates³¹. The two dashed cyan lines show the locations of the two cusps. (e) Solid colour curves and plus signs show the calculated plasma inflow (orange) and outflow (cyan) velocities (left scale) as a function of time. Plus signs indicate that only a single velocity value was obtained. The black solid line shows the calculated magnetic reconnection rate ($M = V_{in}/V_{out}$) with time. Arrows indicate direction of likely uncertainty due to the uncertain final inflow velocity and/or initial outflow velocity.

Fig. 4. The plasma flows and X-ray sources in the reconnection region. The area covered by these plots is indicated by the white box in Fig. 1 and is rotated by 114° to match Fig. 2. This figure shows the curved, expanding inflow loops and the energy release observed in X-rays. (a) Red, green, and blue represent difference AIA images at 171, 193 and 131 Å, respectively, relative to those taken 48 s earlier. Only positive changes are shown for clarity. (b) RHESSI 4 – 10 keV X-ray images with the colour code shown in the lower right expressed as the percentage of the peak flux in each image. White contours in the fourth image show X-ray sources in the 10-20 keV range at 10, 20, 40, 60, and 90% of the peak intensity in each image. The arrows indicate the flow velocity vectors from 10 to 80 km s⁻¹ derived using the FLCT method²⁸ from a pair of

AIA images taken 24 s apart at each wavelength. A smoothed image (with a smoothing window of 5×5 pixels) taken 24 s earlier was subtracted as background from the pair of images to better track the motion of coronal loops. See also supplementary movie M5.

Supplementary Materials:

Figures 1

Movies M1-M5

Fig. 1. Flare loops and ribbons observed by SDO/AIA and RHESSI. This figure shows how the flare ribbons (A, B, C, and D) are defined. (a) The AIA image was taken at 131 \AA at 04:25 UT. The red contours show 5, 10, 20, 40, 60, and 90 percent of the maximum in the RHESSI 4-10 keV X-ray image for the period from 04:22 to 04:26 UT. They show the EUV and X-ray emission from the hot flaring loops. (b) AIA 1600 \AA image and RHESSI 10-20 keV contours showing emission from the flare ribbons/footpoints.

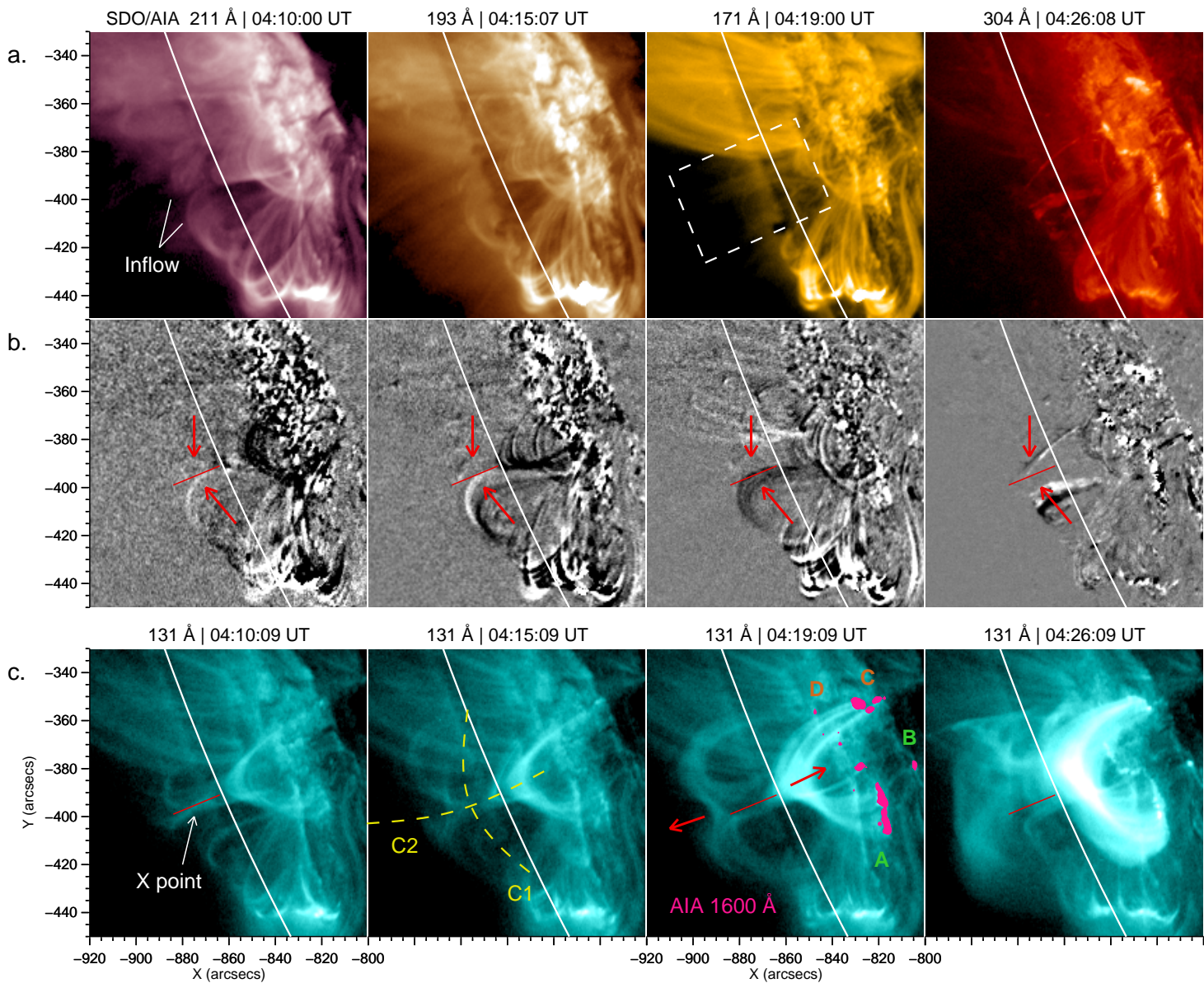
Movie M1. Inflow loops observed by SDO/AIA at 171, 193 and 304 \AA on August 17, 2011. The top row shows the original images taken by AIA. The bottom row shows filtered images of the top row to better indicate the loops. These filtered images are obtained by subtracting a smoothed image from the original image.

Movie M2. SDO/AIA observations of the hot, newly formed loops at 131 \AA on August 17, 2011. The left image is taken by AIA. The image on the right shows a filtered image.

Movie M3. Combined images showing the reconnection process observed at AIA 171, 193, and 131 \AA on August 17, 2011. The left image shows plasma with different temperatures in red (171 \AA), green (193 \AA) and blue (131 \AA). The image on the right shows the running ratio difference images from the same three channels relative to the images taken two minutes earlier. Only positive changes are shown for clarity.

Movie M4. SDO/AIA and RHESSI observations of the energy release on August 17, 2011. The red contours (10, 20, 40, 60, and 90 percent of the maximum) indicate emission at 4-10 keV and the blue at 10-20 keV.

Movie M5. A close look at the reconnection region indicated in Fig. 1. The first three images show the region taken at AIA 171, 193 and 131 \AA . The fourth and fifth images show base difference images and running difference images from the same three channels in different colors (red, green and blue, respectively). These combined images show how cool loops come together horizontally and then disappear and how hot loops form and then separate vertically.



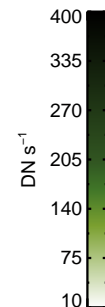
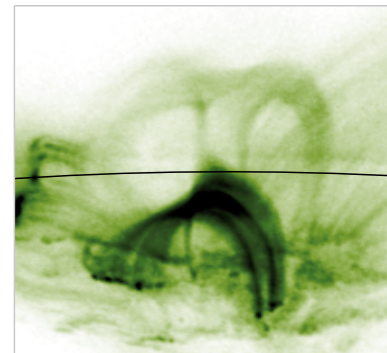
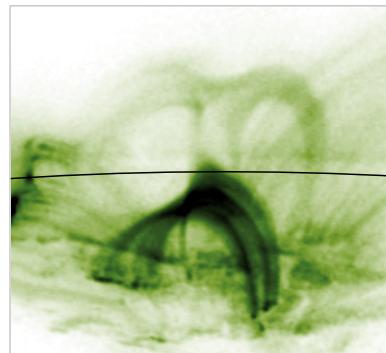
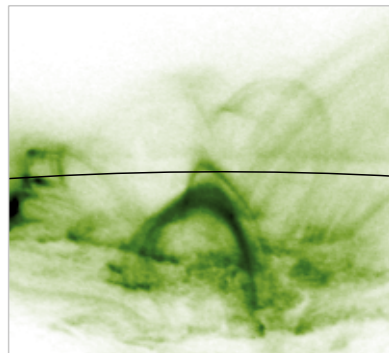
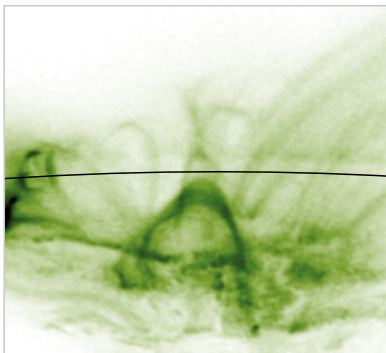
17-Aug-2011 04:10 UT

04:15 UT

04:19 UT

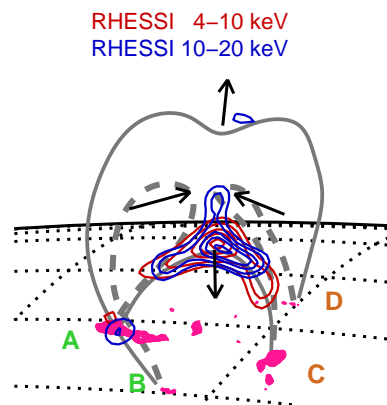
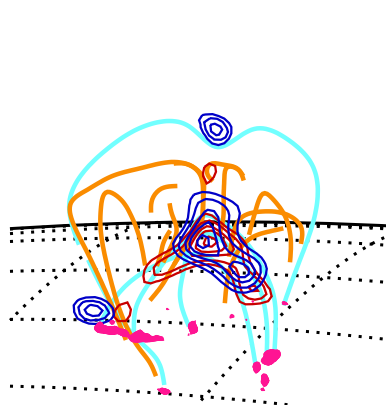
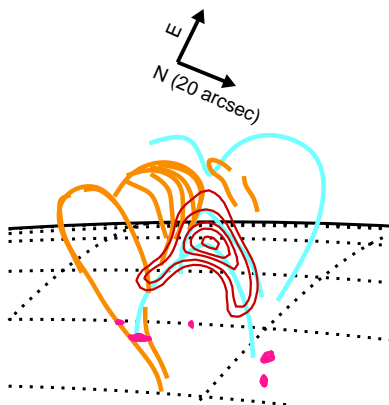
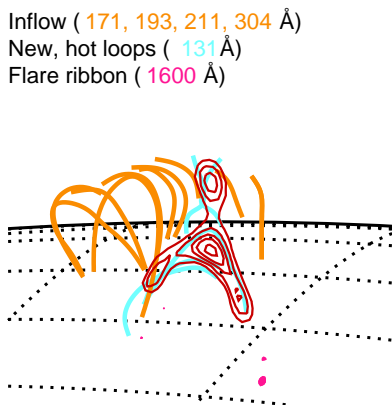
04:20 UT

a. SDO/AIA 131 Å

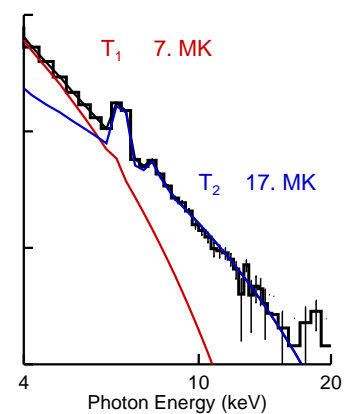
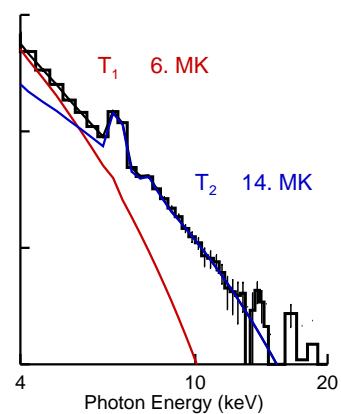
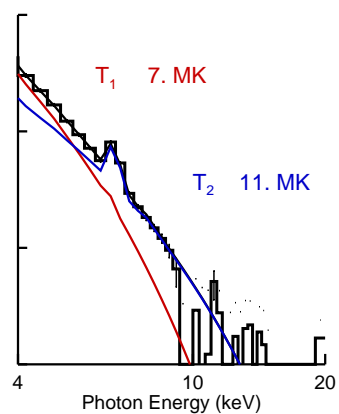
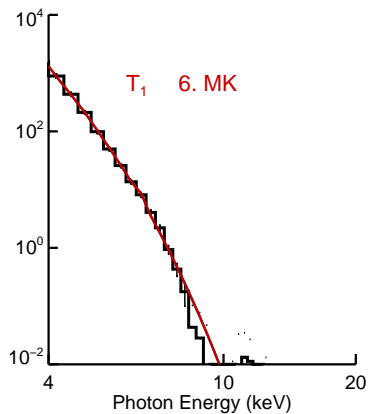


b. RHESSI X-rays images

Inflow (171, 193, 211, 304 Å)
 New, hot loops (131 Å)
 Flare ribbon (1600 Å)

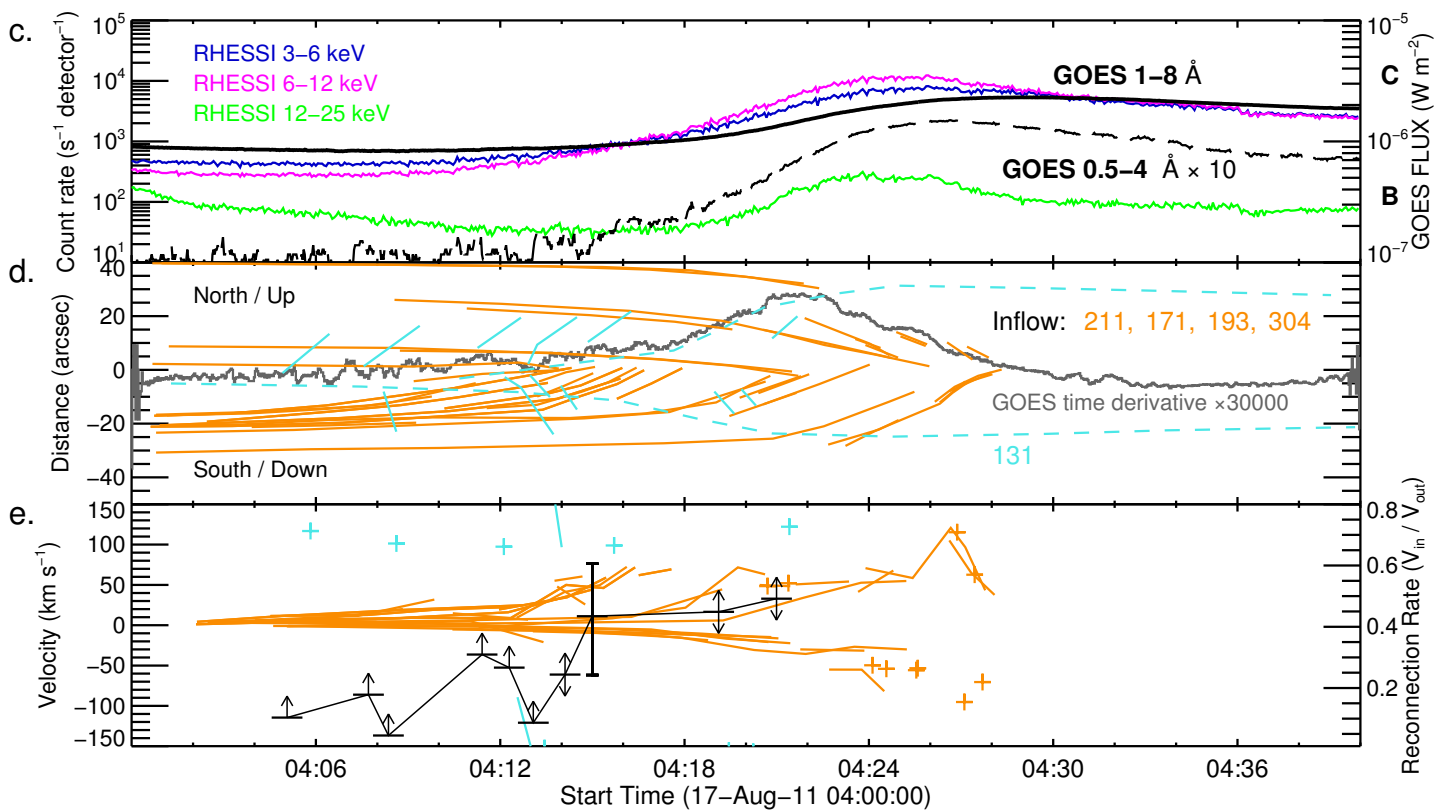
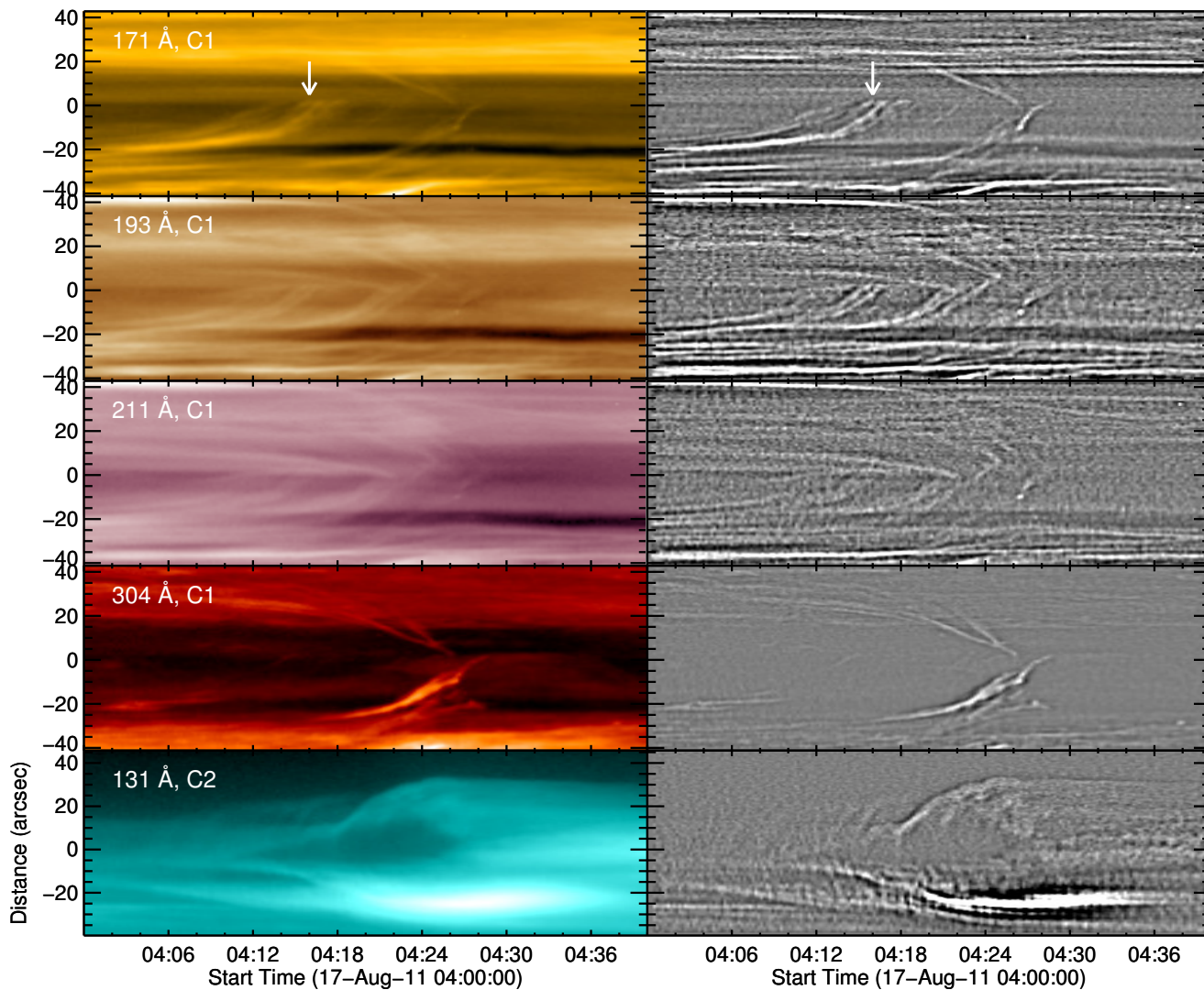


c. RHESSI X-ray spectra

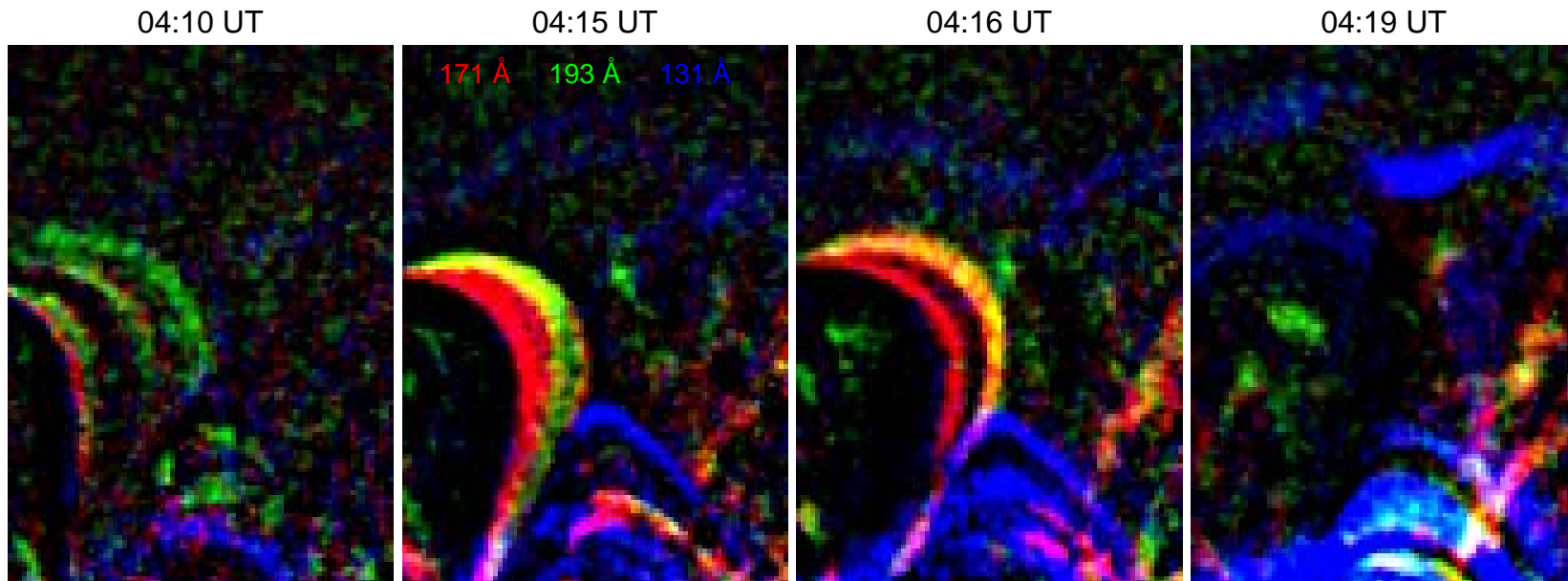


a. Time–distance plots for Curve 1 and 2

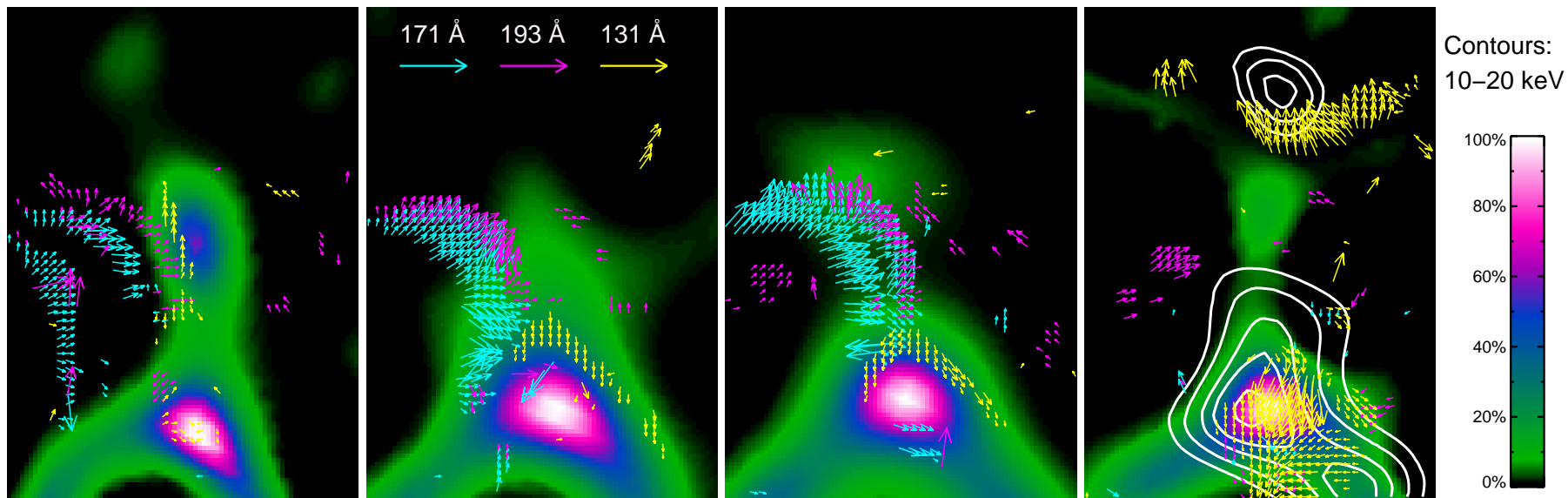
b. Filtered time–distance plots



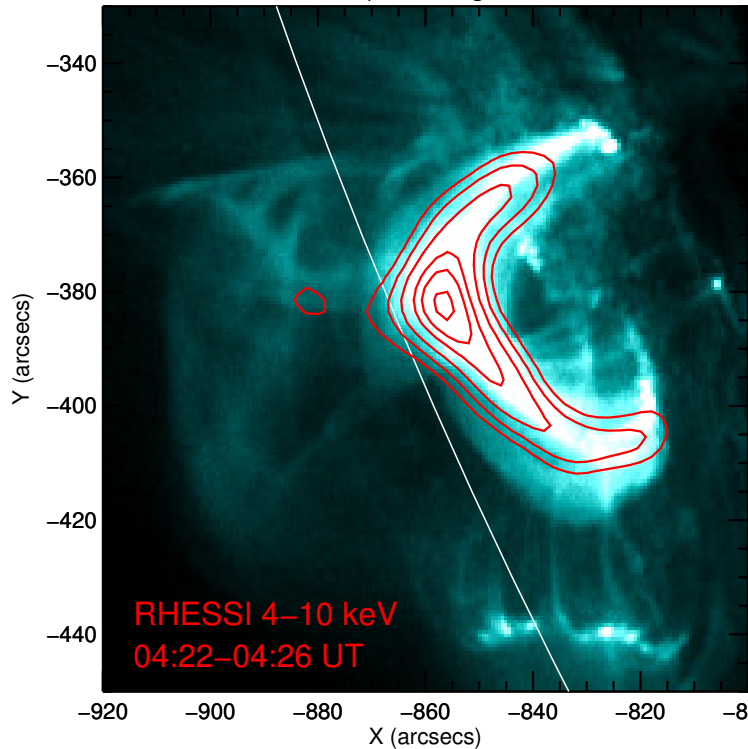
a. SDO/AIA difference images



b. RHESSI images in 4–10 keV



a. SDO/AIA 131 Å | 17-Aug-2011 04:25:10 UT



b. SDO/AIA 1600 Å | 17-Aug-2011 04:25:05 UT

